6-GHz lattice response in a quantum spin-orbital liquid probed by time-resolved resonant x-ray scattering

Kou Takubo,[1,2,*] Takashi Mizokawa,[3] Huiyuan Man,[1,4] Kohei Yamamoto,[1] Yujun Zhang,[1] Yasuyuki Hirata,[1] Hiroki Wadati,[1,5] Daniel I. Khomskii,[6] and Satoru Nakatsuji[1,4,7]

[1]*Institute for Solid State Physics, University of Tokyo, Kashiwa, Chiba 277-8581, Japan*
[2]*Department of Chemistry, Tokyo Institute of Technology, Meguro, Tokyo 152-8551, Japan*
[3]*Department of Applied Physics, Waseda University, Okubo, Tokyo 277-8581, Japan*
[4]*Institute for Quantum Matter and Department of Physics and Astronomy, Johns Hopkins University, Baltimore, Maryland 21218, USA*
[5]*Graduate School of Material Science, University of Hyogo, Koto, Hyogo 678-1297, Japan*
[6]*II Physikalisches Institut, Universität zu Köln, Zülpicher Strasse, 50937 Köln, Germany*
[7]*Department of Physics, University of Tokyo, Hongo, Tokyo 113-0033, Japan*

(Received 4 February 2020; revised 20 June 2021; accepted 28 October 2021; published 10 November 2021)

Long-sought quantum spin liquids usually emerge in geometrically frustrated magnets. Less commonly, unfrustrated magnets can harbor a variety of quantum spin liquids if charge and/or orbital degrees of freedom are involved. Jahn-Teller distortion of $Cu^{2+}O_6$ octahedra is absent in hexagonal $Ba_3CuSb_2O_9$ suggesting a Cu 3*d* spin-orbital liquid state. Here, by means of time-resolved resonant x-ray scattering, we show that hexagonal $Ba_3CuSb_2O_9$ exhibits a charge-orbital dynamics which is absent in the orthorhombic phase of $Ba_3CuSb_2O_9$ with Jahn-Teller distortion and Cu 3*d* orbital order. The time scale of charge-orbital dynamics manifests in the coherent phonons at 6 GHz. The present work reveals a role of electron-lattice entanglement in the quantum spin-orbital liquid state.

DOI: 10.1103/PhysRevB.104.205110

I. INTRODUCTION

Mott insulators with $S = 1/2$ or $J = 1/2$ are expected to show a variety of quantum spin liquid states when magnetic orders are suppressed due to geometrical frustration and/or quantum fluctuation [1–3]. Among them, $RuCl_3$ with a $Ru^{3+}(J = 1/2)$ hexagonal lattice exhibits a Kitaev spin liquid state under magnetic field due to Majorana quantization [4–9]. The Kitaev state can be realized by the strong spin-orbit interaction of 4*d* or 5*d* transition-metal ions on the hexagonal lattice [7]. Another quantum spin liquid state on a hexagonal lattice is realized in $Ba_3CuSb_2O_9$ with $Cu^{2+}(S = 1/2)$ [10,11]. The spin liquid phase in $Ba_3CuSb_2O_9$ can be associated with fluctuations in the orbital sector [12–15] in contrast to the Kitaev state where the orbital degeneracy is lifted due to the strong spin-orbit interaction.

The octahedrally coordinated Cu^{2+} with $3d^9$ electronic configuration (one hole in the tenfold Cu 3*d* subshell) is known as one of the Jahn-Teller active ions. Usually, divalent Cu oxides have Jahn-Teller distorted CuO_6 octahedra [16]. When the CuO_6 octahedron is elongated along the *z* axis, which is a fourfold axis of each octahedron, the Cu 3*d* orbital with $x^2 - y^2$ symmetry is destabilized and accommodates the Cu 3*d* hole. $Ba_3CuSb_2O_9$ harbors two competing phases: an orthorhombic phase with Jahn-Teller distorted CuO_6 octahedra and a hexagonal phase with undistorted CuO_6 octahedra [11,17]. The absence of the Jahn-Teller distortion in the hexagonal phase indicates fluctuations of Cu 3*d* orbital symmetry and thus a kind of orbital liquid state. Such fluctuations have been seen in electron spin resonance (ESR) and nuclear magnetic resonance (NMR) measurements on $Ba_3CuSb_2O_9$ [18,19]. An interesting and important question is how the Cu 3*d* orbital sector is involved in the spin-orbital fluctuations and whether the lattice is involved in those.

The basic crystal structure of $Ba_3CuSb_2O_9$ is shown in Figs. 1(a) and 1(b). The hexagonal phase has symmetry of $P6_3/mmc$, while the space group of the orthorhombic phase is *Cmcm*. In the orthorhombic phase, Sb ions (blue balls) occupy isolated octahedra and half of octahedra forming face-sharing dumbbells in an ordered way [Fig. 1(b)]. Cu ions (yellow balls) occupy the other half of dimer octahedra, so that they form the honeycomb lattice in the *ab* plane as shown in Fig. 1(b). In addition, CuO_6 octahedra are strongly distorted due to the Jahn-Teller effect typical for Cu^{2+}. In the hexagonal phase, the occupancy of Cu and Sb in the two metal sites of the Cu-Sb face-sharing dumbbells is 50% as indicated in Fig. 1(a). However, the Cu and Sb ions in the dumbbells have short-range order and keep the honeycomb structure in nanoscale [11,17].

II. EXPERIMENT

Single crystals of $Ba_3CuSb_2O_9$ were grown under oxygen atmosphere from the $BaCl_2$-based flux [17]. Two types of single crystals were obtained, depending on the growth condition. A small addition (9 mol %) of $Ba(OH)_2$ to the $BaCl_2$ flux was found to stabilize single-phase crystals

*takubo.k.ab@m.titech.ac.jp

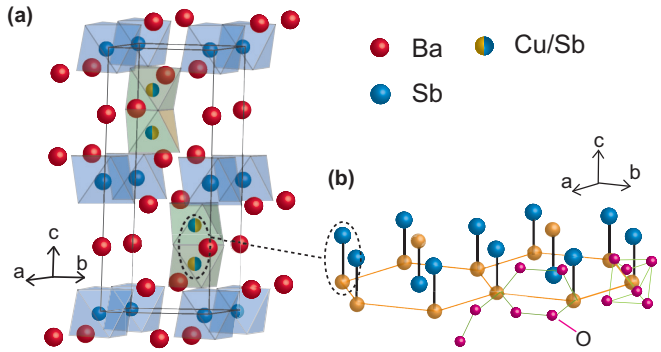

FIG. 1. (a) Schematic crystal structure of hexagonal $Ba_3CuSb_2O_9$. Sb and Cu ions are indicated by blue and yellow, respectively. The space groups of hexagonal and orthorhombic phases at low temperature are $P6_3/mmc$ and $Cmcm$, respectively [11,17]. The occupancy of Cu and Sb in the two metal sites of the Cu-Sb face-sharing dumbbells is 50%. In the orthorhombic phase, the Cu and Sb ions are ordered in the dumbbells and form a honeycomb structure as shown in (b) where the Cu sites are connected by O-O bonds.

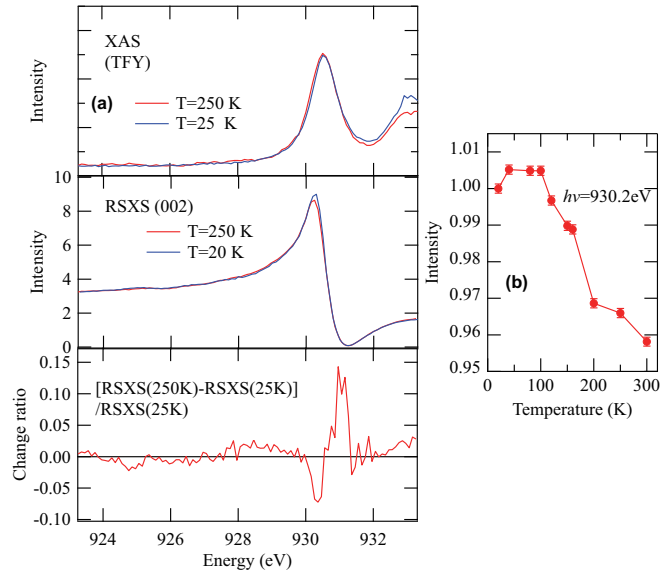

FIG. 2. (a) XAS spectrum in the total fluorescence yield mode and static RSXS spectrum at Q = (002) for hexagonal $Ba_3CuSb_2O_9$ near the Cu L_3 edge ($2p_{3/2}$) taken at 250 and 25 K. The RSXS intensities I(250 K) and I(25 K) are normalized by the intensities of XAS at $h\nu = 923$ eV at 250 and 25 K, respectively, which were simultaneously measured with RSXS. The bottom panel shows the change ratio of $[I(250\text{ K}) - I(25\text{ K})]/I(25\text{ K})$. (b) Temperature dependence of RSXS at $h\nu = 930.2$ eV. The intensity was normalized by the value at $T = 25$ K.

of the hexagonal samples, whereas the pure $BaCl_2$ flux leads to the growth of orthorhombic samples. The composition analysis by inductively coupled plasma atomic emission spectroscopy (ICP-AES) indicates that hexagonal samples are a single phase and are stoichiometric in terms of the Cu-to-Sb elemental ratio [17]. On the other hand, the orthorhombic crystals are rather off-stoichiometric and seemed to contain a part of the inhomogeneous domain of the hexagonal phase. X-ray absorption spectroscopy (XAS) and time-resolved soft x-ray scattering at the Cu L ($2p \rightarrow 3d$) absorption edges were conducted at BL07LSU in SPring-8 [20]. A typical sample size was $150 \times 150 \times 5$ μm^3. The samples were cleaved along the (001) plane *in situ* to avoid surface contamination. The XAS spectra were recorded using both the surface-sensitive total electron yield (TEY) and bulk-sensitive total fluorescence yield (TFY) modes. The time-resolved resonant soft x-ray scattering (RSXS) measurements were performed using the pump-probe technique with a time resolution of ~50 ps [20]. A second-harmonic Ti:sapphire laser pulse ($h\nu =$ 3.1 eV, repetition rate $\simeq$ 1 kHz, full width at half maximum = 50 fs [20,21]) was adopted as the pump light. As a probe light, a synchrotron soft x-ray pulse (full width at half maximum $\simeq$ 50 ps [20,21]) with energy near the Cu L_3 edge was used. The incident x-ray was sigma polarized and parallel to the in-plane (100) crystal axis. The spot size of the x rays and Ti:sapphire laser is approximately 100×50 μm^2 and approximately 600×600 μm^2, respectively. As the area irradiated by the synchrotron x ray is fully exposed by the laser irradiation, the dynamics induced by the laser incidence were probed. By varying the delay time between the x-ray and the laser pulse, time-resolved information was obtained.

III. RESULTS AND DISCUSSION

The soft x-ray diffraction with Q = (002) is structurally allowed and can be accessed in the soft x-ray energy region ($2\theta \sim 135^\circ$ at $h\nu \sim 930$ eV) owing to the long c axis ~15.6 Å of $Ba_3CuSb_2O_9$. Figure 2(a) shows the spectra of XAS and static RSXS around the Cu L_3 edge ($2p_{3/2}$). Here, the polarization of the incident x ray was parallel to (100) of $Ba_3CuSb_2O_9$. The RSXS intensity can generally be formulated as $I = |S(\omega)|^2/\mu(\omega)$, where $S(\omega)$ is the structure factor and given by $S(\omega) = \sum f(\omega)e^{-i\mathbf{Q}\cdot\mathbf{r}}$. Here, $\mu(\omega)$, $f(\omega)$, and $e^{-i\mathbf{Q}\cdot\mathbf{r}}$ are the absorption coefficient, complex dielectric permittivity, and structural component, respectively. Since lattice constant c is less sensitive to the cooperative Jahn-Teller distortion of CuO_6 clusters, the temperature dependence of RSXS at Q = (002) is barely observed below the Cu L_3 resonance of $h\nu < 928$ eV as shown in the bottom panel of Fig. 2(a). On the other hand, the large spectral change is observable around the Cu L_3 resonance of $h\nu \sim 930.2$ eV, reflecting changes in the in-plane dielectric function along (100) of the Cu sites [or $\mu(\omega)$ and $f(\omega)$]. Previous nonresonant in-plane x-ray diffraction (or diffusive scattering) experiments on $Ba_3CuSb_2O_9$ by Ishiguro *et al.* indicated that ferro- and antiferro-orbital fluctuations develop with cooling [18]. The structurally diffusive states are formed at low temperature, and its ferro-orbital correlation saturates below the spin-singlet formation temperature of ~50 K. The temperature dependences of the diffusive scattering around Q = (220) (Fig. 3(e) in Ref. [18]) and of the RSXS at 930.2 eV given in Fig. 2(b) seem to have a similar trend.

Figure 3(a) shows the time-resolved resonant x-ray scattering for Q = (002) at 930.2 eV (on the Cu $2p$ to $3d$ resonance) after the pump pulse at 3.1 eV. A coherent oscillation with period of ~165 ps is clearly observed in the hexagonal phase, while no oscillation is seen in the orthorhombic phase. In addition, the x-ray scattering signals probed at 923.0 eV below

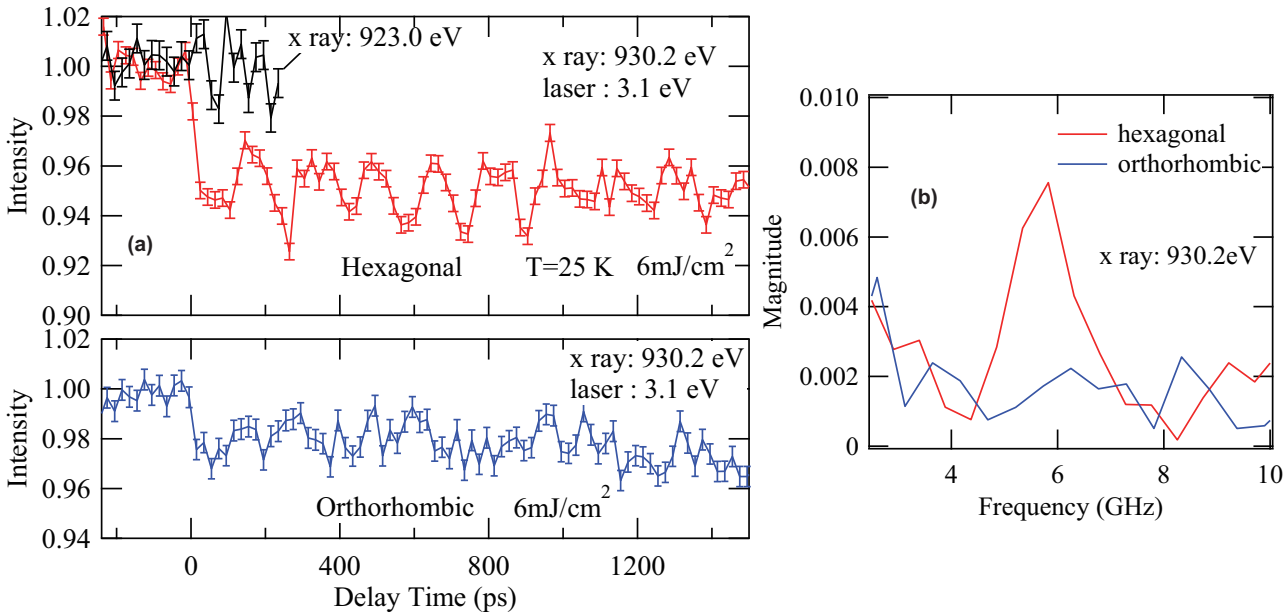

FIG. 3. (a) Photoinduced dynamics at Q = (002) with x ray of 930.2 eV (and 923.0 eV) for the hexagonal and orthorhombic phases after the pump pulse at 3.1 eV. (b) Fourier transform of the time-resolved resonant x-ray scattering signals.

the absorption edge do not show appreciable change after the pump pulse. The static Jahn-Teller distortion of the CuO_6 clusters of the honeycomb lattice of $Ba_3CuSb_2O_9$ scarcely induces the *c*-direction changes, while it provides the *a*-direction changes (elongation of the honeycomb lattice in the *a*-*b* plane due to the cooperative Jahn-Teller effect) as revealed by Katayama *et al.* [17]. Therefore these results clarify that the structural factor along the *c* direction hardly contributes the intensity change of the present x-ray scattering signals. The Fourier transform of the time-resolved data is plotted in Fig. 3(b) indicating that the coherent oscillation corresponds to ∼6 GHz, which is rather slow compared with various optical phonons in the system [17] which are usually coupled to charge or orbital orderings. Such a slow dynamics in the hexagonal phase is consistent with previous reports [18,19]. The time-resolved RSXS signals probed at 930.2 eV could extract these cooperative changes on the electronic states of the Cu sites, which are governed by the temporal evolution of the Cu 3*d* orbital and the Cu-O lattice, whereas the electronic and lattice evolution is triggered by the 3.1-eV laser excitation.

The coherent oscillation with period of ∼165 ps is absent in the orthorhombic sample as shown in Fig. 3(b). Since the pump pulse with 3.1 eV corresponds to the charge transfer excitation from the O 2*p* to Cu 3*d* orbitals [22], the coherent oscillation is related to the charge dynamics in the Cu-O-O-Cu network. The pump excitation at 3.1 eV coherently creates the charge-transferred electronic states with the $d^{10}L$ configuration which have no orbital degrees of freedom. Then the local and temporal Jahn-Teller distortion of the CuO_6 octahedra should be suppressed coherently. When the charge-transferred $d^{10}L$ state is decayed into the d^9 state with a time scale of femtoseconds, the coherent motion of the orbital-lattice coupled units is triggered.

In the quantum spin-orbital liquid state, it has been established that the CuO_6 clusters with Cu 3*d* orbital polarization and Jahn-Teller-type distortion have no static order and are temporally fluctuating with a relatively small frequency of 6 GHz. The 6-GHz oscillation of the Cu 3*d* orbital is consistent with the dynamic Jahn-Teller effect reported in Refs. [18,19]. In Ref. [19], 9 GHz is the lowest frequency available in the experimental setup, and the characteristic 6-GHz oscillation is almost averaged out with the probing frequency of 9 GHz. The orbital and lattice fluctuations correspond to a kind of zero point motion of the orbital-lattice coupled unit which could be made up by single or multiple CuO_6 clusters. In the ground state, the orbital-lattice coupled units are fluctuating with 6 GHz frequency with these fluctuations having different (random) phases. Once the entire system is excited by the coherent pump pulse, coherent vibration of the orbital-lattice coupled units is triggered, and the 6-GHz mode becomes visible and can be probed by RSXS.

On the other hand, in the orthorhombic phase, the Cu sites in the initial state have a static Jahn-Teller distortion, and the distortions are directionally aligned in the macroscopic domains. In this case, the dynamical Jahn-Teller effects on the large cluster with frequency in the gigahertz range should be suppressed. The coherent motion of the Jahn-Teller distortion based on the CuO_6 single cluster may occur in the femtosecond time scale after the pump pulse, as with the coherent phonons reported in ultrafast optical studies for the several orbital-ordered transition-metal oxides. However, such ultrafast motion could not be observed on the present time resolution.

One possible candidate for the orbital-lattice coupled unit in the hexagonal phase is a pair of CuO_6 clusters with ferro-type orbital arrangement [18]. Another candidate would be a hexagonal unit with six CuO_6 clusters. The interaction between neighboring CuO_6 clusters is given through the Cu-O-O-Cu bonds. The neighboring Cu spins are antiferromagnetically coupled for the ferro-type orbital arrangement, while they are ferromagnetically coupled for the antiferro-type orbital arrangement. When the antiferro-

magnetic coupling with the ferro-type orbital arrangement is much stronger than the ferromagnetic one, the orbital-lattice coupled unit would be a pair of neighboring CuO_6 clusters in which the Cu spins form a spin singlet. If this is the case, the orbital and lattice in the two CuO_6 clusters are fluctuating with different phases in the ground state and can form the characteristic frequency. When the ferromagnetic coupling with the antiferro-type orbital arrangement is comparable to the antiferromagnetic one, the unit would be a hexagon with six CuO_6 clusters in which the ferromagnetic and antiferromagnetic bonds are alternatingly arranged. The ferromagnetic and antiferromagnetic arrangements in the hexagons are vibrating with different phases in the ground state and can form the characteristic frequency. The (d^9 to $d^{10}L$) charge transfer excitation by the laser once suppresses the orbital degree of the freedom and breaks the singlet or coupling on the six CuO_6 clusters in the femtosecond time scale. After the photoexcitation, the orbitals will be temporally aligned along the polarization of the pump light and will gradually recover to the random-singlets phase with a vibration of the characteristic frequency for the system of ~6 GHz. Although we cannot determine the unit size from the present RSXS results, the coherently vibrating state after the pump pulse is probably close to the situation illustrated in Fig. 4.

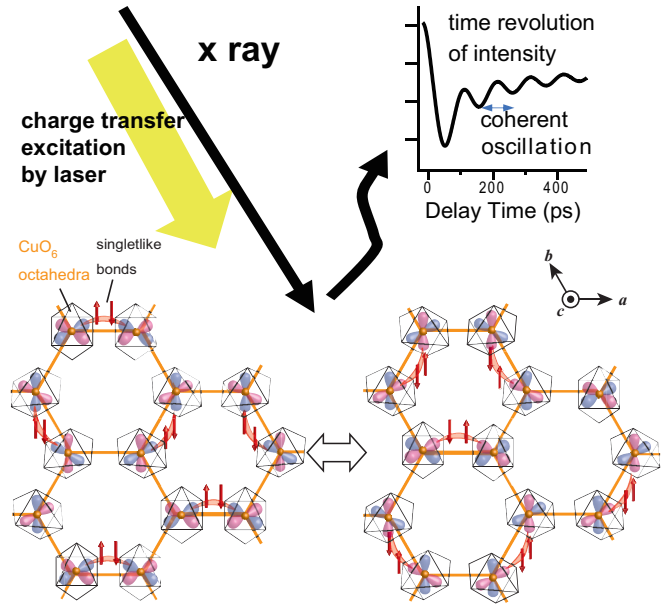

FIG. 4. Schematic picture of photoinduced charge-orbital dynamics in the hexagonal phase. In the initial state of the hexagonal phase, the spin-orbital resonant state or dynamical Jahn-Teller effects for the Cu sites have been suggested. It is believed that the orbitals are not aligned, but form randomly distributed singletlike states through the Cu-O-O-Cu couplings. The red arrows indicate the resonancelike orbital fluctuations proposed by Nasu *et al.* [15], which constitute one of the examples of possible orbital fluctuation mechanisms. Coherent vibration between the possible resonant states is observed, reflecting the characteristic frequency for the system.

IV. CONCLUSION

In conclusion, the coherent oscillations of 6 GHz, clearly observed in pump-probe resonant x-ray scattering, indicate that the spin and orbital fluctuations in the hexagonal phase have relatively slow dynamics and suggest that the spin-charge-orbital fluctuation can be controlled by optical excitation. The coherent oscillation in the pump-probe resonant x-ray scattering measurement suggests that the spin-charge-orbital fluctuation in the hexagons can be controlled by optical excitation. The present result paves an avenue towards optical control of the spin-charge-orbital states in transition-metal compounds with rich physical properties.

ACKNOWLEDGMENTS

We are grateful for fruitful discussions with and support from S. Koshihara and T. Ishikawa. XAS and time-resolved RSXS measurements were performed under the approval of the Synchrotron Radiation Research Organization, The University of Tokyo (No. 2015A7401, No. 2018B7577 and No. 2018B7579). The work of D.I.Kh. is funded by the Deutsche Forschungsgemeinschaft (DFG, German Research Foundation), Project No. 277146847 - CRC 1238. This work was supported by JSPS KAKENHI Grants No. 18K03534 and No. 21K03461.

[1] A. Kitaev, Anyons in an exactly solved model and beyond, Ann. Phys. (Amsterdam) **321**, 2 (2006).

[2] P. A. Lee, An end to the drought of quantum spin liquids, Science **321**, 1306 (2008).

[3] L. Balents, Spin liquids in frustrated magnets, Nature (London) **464**, 199 (2010).

[4] S.-H. Do, S.-Y. Park, J. Yoshitake, J. Nasu, Y. Motome, Y. S. Kwon, D. T. Adroja, D. J. Voneshen, K. Kim, T.-H. Jang, J.-H. Park, K.-Y. Choi, and S. Ji, Majorana fermions in the Kitaev quantum spin system α-$RuCl_3$, Nat. Phys. **13**, 1079 (2017).

[5] Y. Kasahara, T. Ohnishi, Y. Mizukami, O. Tanaka, S. Ma, K. Sugii, N. Kurita, H. Tanaka, J. Nasu, Y. Motome, T. Shibauchi, and Y. Matsuda, Majorana quantization and half-integer thermal quantum Hall effect in a Kitaev spin liquid, Nature (London) **559**, 227 (2018).

[6] G. Baskaran, S. Mandal, and R. Shankar, Exact Results for Spin Dynamics and Fractionalization in the Kitaev Model, Phys. Rev. Lett. **98**, 247201 (2007).

[7] G. Jackeli and G. Khaliullin, Mott Insulators in the Strong Spin-Orbit Coupling Limit: From Heisenberg to a Quantum Compass and Kitaev Models, Phys. Rev. Lett. **102**, 017205 (2009).

[8] J. Knolle, D. L. Kovrizhin, J. T. Chalker, and R. Moessner, Dynamics of a Two-Dimensional Quantum Spin Liquid: Signatures of Emergent Majorana Fermions and Fluxes, Phys. Rev. Lett. **112**, 207203 (2014).

[9] J. Nasu, M. Udagawa, and Y. Motome, Thermal fractionalization of quantum spins in a Kitaev model: Temperature-linear specific heat and coherent transport of Majorana fermions, Phys. Rev. B **92**, 115122 (2015).

[10] H. D. Zhou, E. S. Choi, G. Li, L. Balicas, C. R. Wiebe, Y. Qiu, J. R. D. Copley, and J. S. Gardner, Spin Liquid State in the $S = 1/2$ Triangular Lattice $Ba_3CuSb_2O_9$, Phys. Rev. Lett. **106**, 147204 (2011).

[11] S. Nakatsuji, K. Kuga, K. Kimura, R. Satake, N. Katayama, E. Nishibori, H. Sawa, R. Ishii, M. Hagiwara, F. Bridges, T. U. Ito, W. Higemoto, Y. Karaki, M. Halim, A. A. Nugroho, J. A. Rodriguez-Rivera, M. A. Green, and C. Broholm, Spin-orbital short-range order on a honeycomb-based lattice, Science **336**, 559 (2012).

[12] L. F. Feiner, A. M. Oles, and J. Zaanen, Quantum Melting of Magnetic Order due to Orbital Fluctuations, Phys. Rev. Lett. **78**, 2799 (1997).

[13] Y. Li, Q. Ma, M. D. N. Shi, and F. C. Zhang, SU(4) Theory for Spin Systems with Orbital Degeneracy, Phys. Rev. Lett. **81**, 3527 (1998).

[14] F. Vernay, K. Penc, P. Fazekas, and F. Mila, Orbital degeneracy as a source of frustration in $LiNiO_2$, Phys. Rev. B **70**, 014428 (2004).

[15] J. Nasu, A. Nagano, M. Naka, and S. Ishihara, Doubly degenerate orbital system in honeycomb lattice: Implication of orbital state in layered iron oxide, Phys. Rev. B **78**, 024416 (2008).

[16] D. I. Khomskii, *Transition Metal Compounds* (Cambridge University Press, Cambridge, 2014).

[17] N. Katayama, K. Kimura, Y. Han, J. Nasu, N. Drichko, Y. Nakanishi, M. Halim, Y. Ishiguro, R. Satake, E. Nishibori, M. Yoshizawa, T. Nakano, Y. Nozue, Y. Wakabayashi, S. Ishihara, M. Hagiwara, H. Sawa, and S. Nakatsuji, Absence of Jahn-Teller transition in the hexagonal $Ba_3CuSb_2O_9$ single crystal, Proc. Natl. Acad. Sci. USA **112**, 9305 (2015).

[18] Y. Ishiguro, K. Kimura, S. Nakatsuji, S. Tsutsui, A. Q. R. Baron, T. Kimura, and Y. Wakabayashi, Dynamical spin-orbital correlation in the frustrated magnet $Ba_3CuSb_2O_9$, Nat. Commun. **4**, 2022 (2013).

[19] Y. Han, M. Hagiwara, T. Nakano, Y. Nozue, K. Kimura, M. Halim, and S. Nakatsuji, Observation of the orbital quantum dynamics in the spin-1/2 hexagonal antiferromagnet $Ba_3CuSb_2O_9$, Phys. Rev. B **92**, 180410(R) (2015).

[20] K. Takubo, K. Yamamoto, Y. Hirata, Y. Yokoyama, Y. Kubota, S. Yamamoto, S. Yamamoto, I. Matsuda, S. Shin, T. Seki, K. Takanashi, and H. Wadati, Capturing ultrafast magnetic dynamics by time-resolved soft x-ray magnetic circular dichroism, Appl. Phys. Lett. **110**, 162401 (2017).

[21] S. Yamamoto and I. Matsuda, Time-resolved photoelectron spectroscopies using synchrotron radiation: Past, present, and future, J. Phys. Soc. Jpn. **82**, 021003 (2013).

[22] K. Takubo, H. Man, S. Nakatsuji, K. Yamamoto, Y. Zhang, Y. Hirata, H. Wadati, A. Yasui, T. Mizokawa, and D. I. Khomskii, Spin-orbital liquid in $Ba_3CuSb_2O_9$ stabilized by oxygen holes, Phys. Rev. Materials **5**, 075002 (2021).